The Effect of Niobium on the Hardenability of Microalloyed Austenite

C. FOSSAERT, G. REES, T. MAURICKX, and H.K.D.H. BHADESHIA

The powerful effect that varying the extent of niobium-carbide dissolution has on the "hardenability" of microalloyed austenite is demonstrated using dilatometric measurement of the critical cooling rate required to from microstructures containing >95 pct martensite. The results can be rationalized on the hypothesis that the hardenability of austenite is enhanced by niobium in solid solution, possibly by its segregation to austenite grain boundaries, but is decreased by precipitation of niobium-carbide particles. This effect appears analogous to that of boron in steels and is found to be independent of variations in the austenite grain size.

I. INTRODUCTION

SEVERAL models exist for the calculation of the microstructure in the heat-affected zone of steel welds.[1,2,3] There is also research that enables the dissolution kinetics of microalloying elements such as niobium to be estimated.[4,5] The results have been used previously to improve the austenite-grain-size calculations for the heat-affected zone on the basis that precipitates pin the grain boundaries and hence influence grain size. However, there is evidence that the precipitation or dissolution of carbides in microalloyed steels have effects beyond those expected just from the pinning effect.[6–10] The kinetics of ferrite formation appear to be retarded even though the concentration of niobium might be very small indeed.

The purpose of the present work was to verify that a microalloyed steel containing niobium undergoes detectable changes in hardenability as a function of heat treatments designed to alter the distribution of niobium between the austenite and carbides.

II. MATERIALS

The steel used for most of the experimental work was a low-carbon normalizing steel with a microalloying addition of niobium. An additional alloy with a similar chemistry but without niobium was also studied for comparison purposes. The chemical compositions of the two steels (labeled steel 1 and steel 2, respectively) are given in Table I. Whereas it was anticipated that niobium would form carbonitride compounds in steel 1, it was assumed here that precipitates would be predominantly carbides, and the term niobium carbide is used throughout this work.

A. *Dilatometry*

Simulation experiments were performed on a Gleeble 1500 (Duffers Instruments) or a Thermechmastor thermomechanical (Fuji Electric) simulator with computer control and data acquisition. Both are capable of monitoring the transformations as they happen *via* the accompanying dimensional changes, using laser (Thermechmastor) or mechanical (Gleeble) transducers. Both simulators used cylindrical samples, of dimensions 5 × 70 mm for the Gleeble and 8 × 12 mm for the Thermechmastor.

A diagram illustrating the typical form of the heat treatments used for the experiments is given in Figure 1. The thermal cycle parameters of interest are the austenitization time (t_γ) and temperature (T_γ), the cooling rate (V_{int}) through the intermediate temperature range 980 °C to 750 °C, and the cooling rate from 750 °C to room temperature (V_f). For a given series of thermal cycles, as the austenitization temperature was varied, the duration of the hold at the peak temperature was adjusted so that the total time spent above 980 °C was the same in all cases. With the extremely rapid heating and cooling between 980 °C and the hold temperature, the thermal cycles therefore approximated isothermal holds at T_γ. Consequently, throughout this work, the term t_γ refers to the total time spent by the sample at temperatures in excess of 980 °C.

For the variety of heat treatments studied, the parameter identified to represent the hardenability of the austenite was chosen to be the critical cooling rate required to produce a microstructure with a martensite fraction greater than 0.95. The martensite-start (M_s) temperature of the steel was determined dilatometrically to be 430 °C, which was confirmed by metallography. For a given cooling rate, the amount of austenite present in the microstructure at any instant is then obtained from the dilatometric curve by comparing the instantaneous dimension of the sample relative to the limiting dimensions when the sample is fully austenitic or fully ferritic. The latter cases are represented at any temperature by extrapolating the high and low temperature ends of the dilatometric curve, respectively; the procedure is illustrated in Figure 2. If it is reasonably assumed that after martensitic transformation the amount of austenite that is retained at room temperature can be neglected, then the fraction of martensite is identical to that of austenite at the M_s temperature of the austenite. From a continuous-cooling transformation (CCT) curve plot for 5 pct transformation, the critical cooling rate is determined by interpolation between cooling rates at which this curve

C. FOSSAERT, Engineering Student, Université de Technologie de Compiègne, and T. MAURICKX, Research Engineer, are with SOLLAC, Dunkerque, France. G.I. REES, Research Associate, and H.K.D.H. BHADESHIA, Reader in Physical Metallurgy, are with the Department of Materials Science and Metallurgy, University of Cambridge, Cambridge CB1 3Q2, United Kingdom.

Manuscript submitted November 24, 1993.

Table I. Chemical Compositions (Wt Pct) of the Experimental Steels

	C	Mn	Si	Nb	N
Steel 1	0.152	1.545	0.467	0.035	0.0053
Steel 2	0.178	1.527	0.023	—	0.0037

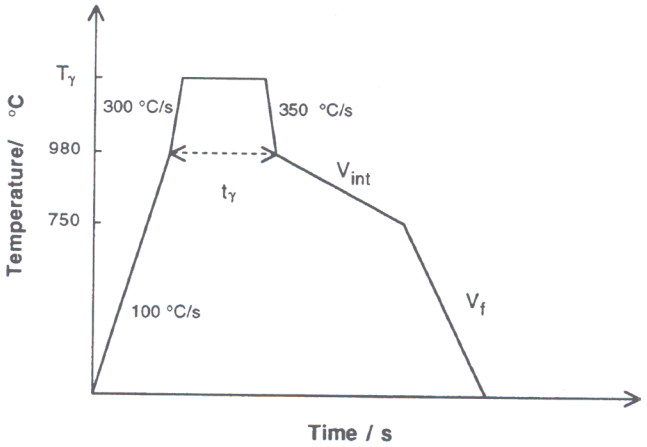

Fig. 1 — Illustration of the heat treatments studied. The term t_γ refers to the total time spent by the specimen above 980 °C.

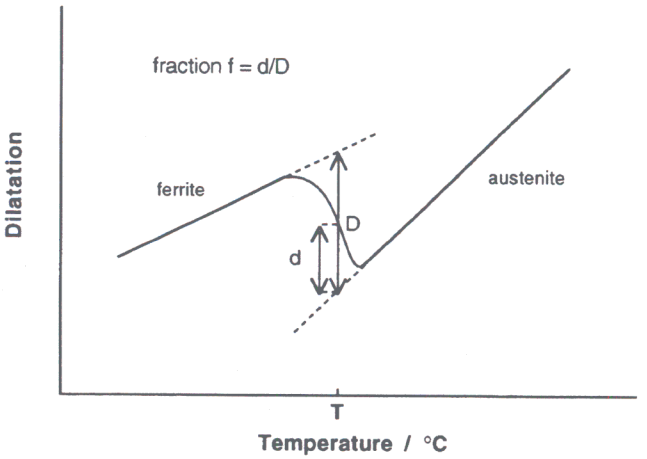

Fig. 2 — Illustration of the graphical method of determining the ferrite fraction f formed at temperature T from analysis of dilatometric data.

crosses the M_s temperature. A comparison between experimental dilatometric curves giving 100 and 90 pct martensite is given in Figure 3.

III. METALLOGRAPHY

Selected specimens were chosen for detailed metallographic examination. These were ground and polished by standard techniques and etched in accordance with the information required. For austenite grain size determination, the etchant was aqueous picric acid with teepol, which is a wetting agent. For examination of the microstructure using scanning electron microscopy (SEM), 2 pct nital was used.

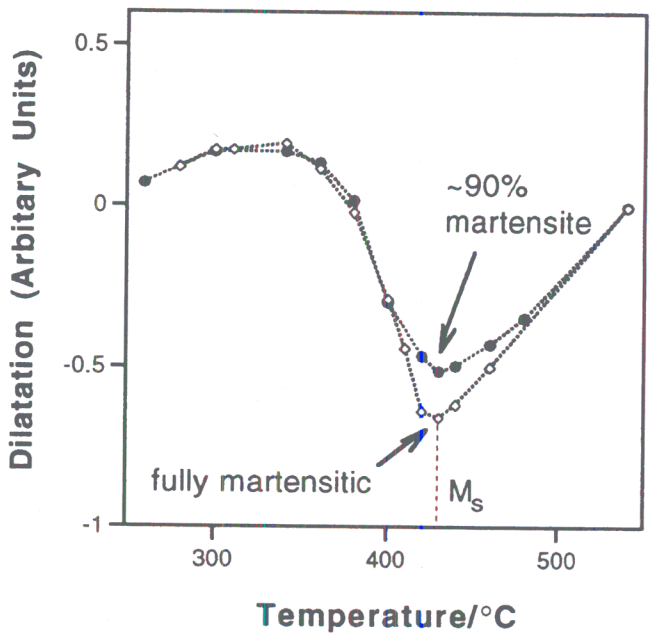

Fig. 3 — Illustration of dilatometric curves for cooling rates giving 100 pct and 90 pct martensite in the microstructure.

IV. THE DISSOLUTION OF NIOBIUM CARBIDE

An established and convenient method for estimating the dissolution temperature of precipitate particles subjected to thermal cycles of the type experienced by weld-heat-affected zones has been proposed by Ashby and Easterling.[15] The matrix is divided into cells, each of which is associated with a particular particle. The part of each region that can participate in the carbide dissolution process is assumed to be bounded by a surface of radius equal to the diffusion distance of the slowest diffusing species. This diffusion distance varies parabolically with time, and its magnitude is also determined by the diffusivity of the species so that the model contains both time and temperature. Thermodynamics only enters *via* a temperature-dependent solubility product, which ensures that complete dissolution is only possible if, at any instant of time, the solubility of niobium in the matrix is equal to or in excess of the overall concentration of niobium. Details of the method are presented in the Appendix. The calculations require an estimate of the volume l^3 of matrix associated with each carbide particle, *i.e.*, this volume effectively defines the particle size. Maurickx[111] has measured

$$l = 10^{-7}\ \text{m}$$

for a normalized steel of similar composition. In order to verify the predicted dissolution kinetics of the carbide, the amount of niobium present as precipitates after different thermal cycles was determined by chemical analysis of extracted particles in the laboratories of IRSID Unieux (St. Germaine-en-Laye, France). Extraction was achieved by dissolving the steel matrix in a citric acid solution, with the particles then being separated by filtration (pore size = 0.04 μm), which put a lower limit of 10 nm on the extracted particle size. After dissolving

the filtered particles in sulfuric acid, the niobium content was quantified by flame spectrometry. In this way, the amount of niobium *in precipitated form* was determined for each thermal cycle listed.

V. RESULTS

A. *Phase Calculations*

Table II gives the temperature ranges of stability of ferrite, austenite, and niobium carbide (NbC) calculated by the Thermocalc[12] phase diagram modeling software package, using the iron-based "Fe" database.

B. *The Dissolution of Niobium Carbide*

The results of the chemical analysis of the extracted particles are displayed in Table III. The thermal cycles applied to the test specimens are shown schematically in Figure 4. The heating rate to the maximum temperature was 100 °C s^{-1}, followed either by direct cooling to room temperature at 100 °C s^{-1} or by an isothermal hold, of duration Δt_γ at the highest temperature, before cooling. The effect of cooling at 0.5 °C s^{-1} between 980 °C and a variable intermediate temperature T_2 was also investigated. Because it is the amount of niobium in precipitate form that is measured, the concentration in solid solution is deduced by difference from the total content. This assumes that all the niobium is present in carbide form in the (normalized) as-received steel.

A plot of the niobium concentration in solid solution *vs* the austenitization temperature is shown in Figure 5. There was no hold at the peak temperature for these cycles. Despite some scatter, the points are in good agreement with the equilibrium niobium concentrations, predicted by the solubility product relationship of Perdrix *et al.*,[13] which accounts for the presence of manganese in the steel. It is apparent that even at a heating rate of 100 °C s^{-1} niobium carbide/austenite equilibrium is established rapidly above 1050 °C. For this heating rate, *predicted* dissolution curves are shown in Figure 6, following the model outlined in the Appendix. The predicted dissolution kinetics of the carbides depend strongly on the volume of the matrix cell into which they dissolve, and hence on the particle size. Calculations are shown for matrix cell radii of l = 7, 8, and 9 × 10^{-8} m per particle. For this heating rate, the model indicates that the need for superheating above 1100 °C becomes negligible for $l \leq 7 \times 10^{-8}$ m. Using this cell radius, we have verified by calculation that the thermal cycles illustrated in Figure 1 cause equilibration of niobium concentration during the isothermal hold at the maximum temperature, even for T_γ = 980 °C. It is interesting to note the degree of agreement between the predictions of the Thermocalc software package with those of Perdrix *et al.* Figure 7 shows that there are significant differences between the two as the temperature of complete dissolution is approached.

Table III also shows that the effect of cooling slowly through the temperature range of 980 °C through 750 °C on the amount of niobium in solid solution is negligible, indicating that there is no *bulk* precipitation of carbides during this stage of the thermal cycle.

Table II. Temperature Ranges of Phase Stability for Steels 1 and 2 for Austenite (γ), Ferrite (α), and Niobium Carbide (NbC)

Alloy	Phase Boundary	
	(α + γ + NbC)/(γ + NbC)	(γ + NbC)/γ
Steel 1	824 °C	1195 °C
Alloy	Phase boundary	
	(α + γ)/γ	
Steel 2	796 °C	

C. *Effect of Austenite Grain Size on V_c*

In order to compare the critical cooling rate of specimens with different austenite grain sizes, specimens of both steels were subjected to thermal cycles with a fixed intermediate cooling rate of V_{int} = 100 °C s^{-1} in which T_γ was varied. This high cooling rate ensures that carbides do not precipitate from the austenite within the intermediate temperature range.

The critical cooling rate for a martensite fraction of 0.95 was determined for each condition. In all cases, the time spent by the sample at temperatures above 980 °C during austenitization was fixed at 8 seconds. The austenite grain size index was determined by comparison of optical micrographs with standard grain size charts.[14]

Figure 8 compares the measured austenite grain sizes for steels 1 and 2 as functions of the austenitization temperature. The grain-growth behavior is very different in the two cases. Steel 1 shows the classic behavior of a niobium microalloyed steel in that the grain growth is limited until the temperature of carbide dissolution is reached. After this temperature is surpassed, the grain-boundary pinning effect vanishes as the particles dissolve completely, leading to rapid austenite grain growth. Steel 2, as expected, shows a much smoother variation in the grain size as the austenitization temperature is increased.

Figure 9 shows the relationship between the austenite grain size and the critical cooling rate for steels 1 and 2. It is clear that there is a different relationship between austenite grain size and critical cooling rate for the two alloys. For the niobium-containing steel 1, the results of modeling the dissolution of niobium-carbide particles during the thermal cycles are shown in Figure 10. There is a clear relationship between the calculated concentration of dissolved niobium and the measured critical cooling rate. The critical cooling rate for martensite formation significantly decreases as the carbides dissolve, and niobium is returned into solid solution. As the austenitization temperature is increased, three factors may contribute to the increase in hardenability, namely, the increase in austenite grain size, the increasing concentration of niobium in solution, and the decrease in the fraction of niobium carbide in the austenite. Figure 9, however, shows that a dramatic increase in hardenability for steel 1 occurs over a range of very little austenite grain growth and that once significant grain growth does occur, the critical cooling rate does not change very much.

Table III. Thermal Cycle Details and Results of Chemical Analysis of the Dissolution Behavior of Niobium Carbide*

Cycle	Base Metal	A	B	C	D	E	F	G	H	K
T_γ/°C	—	1100	1130	1150	1170	1150	1050	1250	1250	1150
Δt_γ/s	—	0	0	0	0	7	7	7	7	7
T_2/°C	—	—	—	—	—	—	—	750	940	750
$[Nb]_p$/ppm (wt)	310	200	215	115	165	145	235	<50	<50	155
$[Nb]_{ss}$/ppm (wt)	0	110	95	195	145	165	75	310	310	155

*$[Nb]_{ss}$ and $[Nb]_p$ represent the concentration of niobium in solid solution and precipitate form, respectively.

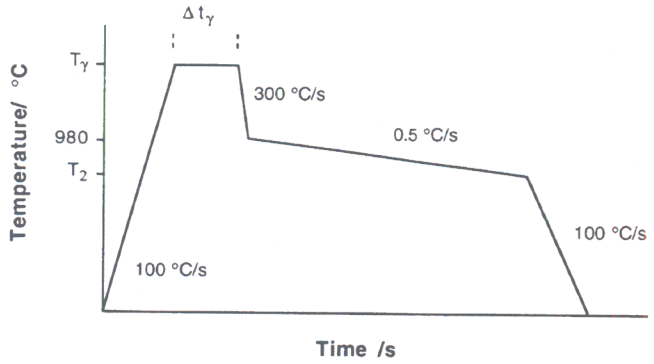

Fig. 4—The thermal cycles used for investigation of the dissolution behavior of niobium carbide. The term Δt_γ denotes the isothermal holding time at the maximum temperature.

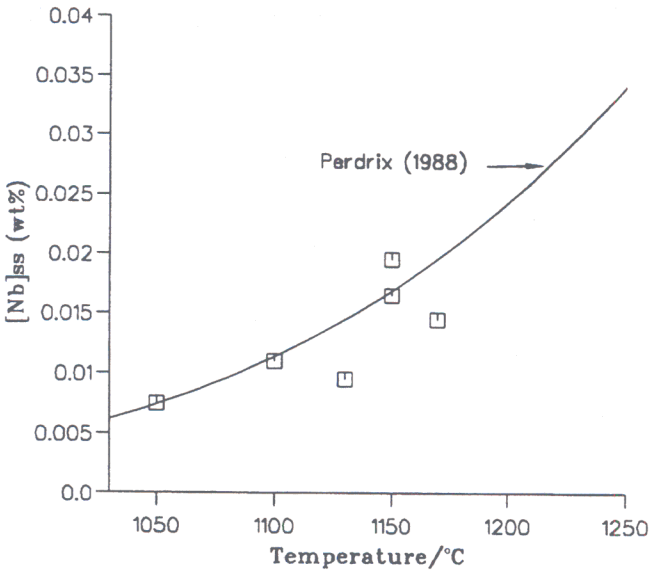

Fig. 5—The experimentally measured values of the dissolved-niobium content of Steel 1 as a function of peak temperature T_γ, for heating at 100 °C s^{-1} and no hold at the peak temperature.

This indicates that for steel 1, the dominant factor affecting the hardenability is not the austenite grain size.

D. *Varying the Intermediate Cooling Rate*

In the intermediate temperature range (980 °C through 750 °C), ferrite does not form, but the austenite is unstable with respect to niobium-carbide precipitation. In all of the experiments presented previously, the cooling

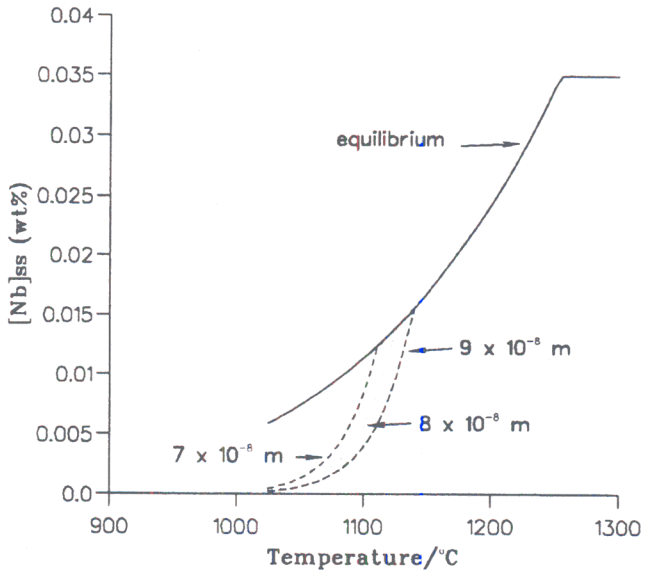

Fig. 6—Predicted values for the dissolved niobium concentration in Steel 1 as a function of temperature. Calculations are shown for a heating rate of 100 °C s^{-1} and for different matrix cell radii l.

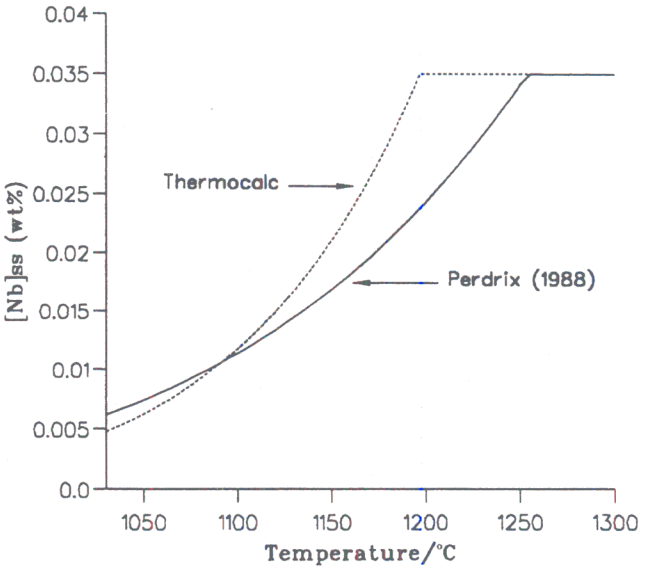

Fig. 7—Comparison of the equilibrium concentration of niobium in solid solution as a function of temperature according to the predictions of Thermocalc and the solubility product relationship of Ref. 13.

rate through this temperature range was rapid and constant in order to avoid any possible carbide precipitation below 980 °C. Further experiments were conducted in which the austenitization temperature and time were fixed but V_{int} was varied in order to investigate possible precipitation effects while maintaining a constant austenite grain size.

After austenitization with T_γ = 1250 °C and t_γ = 8 seconds, the effect of varying V_{int} between 100 °C s^{-1} and 0.5 °C s^{-1} was investigated. The austenitization treatment was confirmed by calculation to be capable of *completely* dissolving all niobium-carbide particles. Any effects arising from varying V_{int} should therefore be attributable to the segregation of niobium and carbon and/or the precipitation of niobium carbide.

Figure 11 clearly demonstrates the dramatic effect that varying V_{int} has on the critical cooling rate for the formation of the prescribed amount of martensite. In particular, the effect is most noticeable for V_{int} between 0.5 °C s^{-1} and 10 °C s^{-1}. At higher values of V_{int}, the effect decreases significantly. As V_{int} is varied, an extremely close correlation is observed between V_c and the

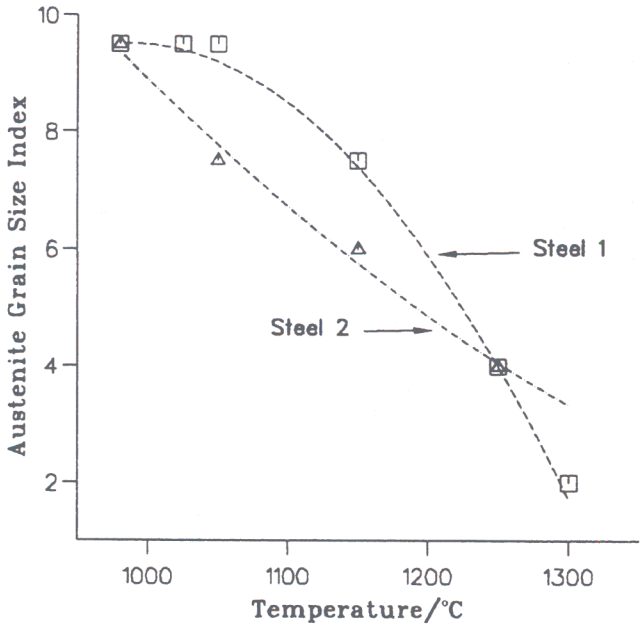

Fig. 8—The variation of austenite grain size with temperature for Steels 1 and 2. Note that a larger grain-size index corresponds to a small austenite grain size. The total time spent above 980 °C in all cases was 8 s.

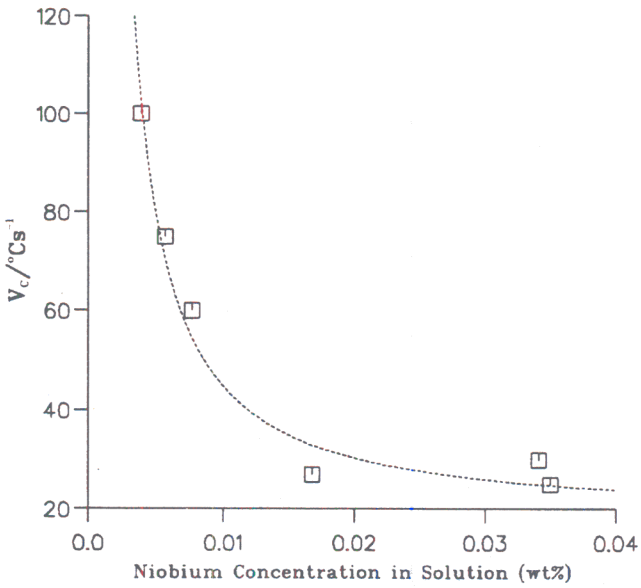

Fig. 10—The critical cooling rate as a function of the calculated concentration of niobium in solution for Steel 1.

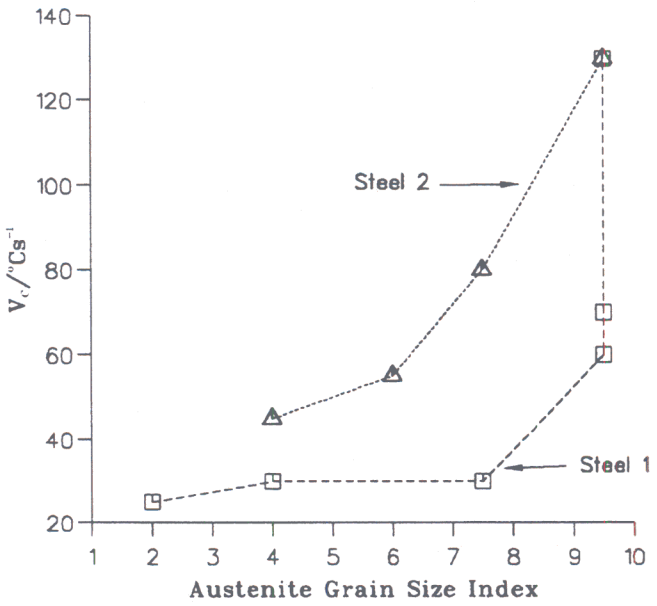

Fig. 9—The relationship between the critical cooling rate necessary to obtain a fraction 0.95 of martensite, and the austenite grain size for Steels 1 and 2. Steel 2 is niobium-free.

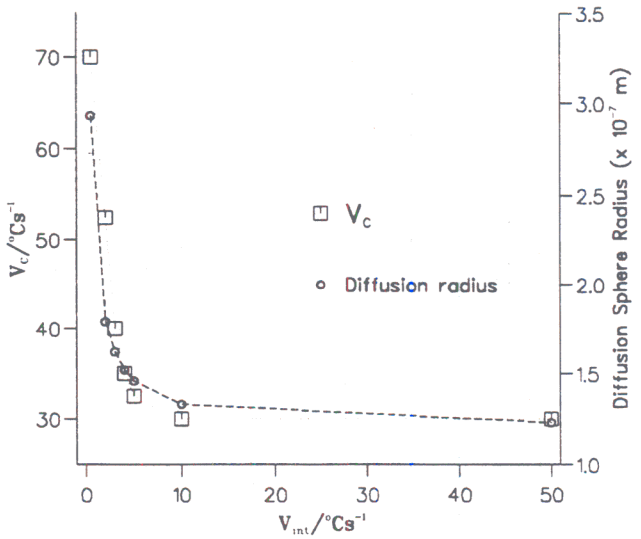

Fig. 11—The effect of varying the cooling rate V_{int} in the intermediate temperature range on the critical cooling rate, and the diffusion distance of niobium after an austenitization treatment with T_γ = 1250 °C and t_γ = 8 s.

distance over which niobium atoms can diffuse during the temperature interval of 980 °C through 750 °C (Figure 11). Chemical analysis of extracted particles indicated, however, that there is no precipitation of carbides from the bulk austenite during this interval. As shown in Figure 11, the distances that niobium atoms can diffuse during this time are greater than the estimated original interparticle spacing. Precipitation during this stage must therefore be limited by the nucleation rate of carbide particles, because there is ample time for the diffusion of niobium through the matrix. Despite this fact, transmission electron microscopy (TEM) on extraction replicas reveal that a small number of niobium carbide precipitates are present in a specimen cooled at 50 °C s^{-1} following a thermal cycle with T_γ = 1300 °C and V_{int} = 0.5 °C s^{-1}. A micrograph of such particles is shown in Figure 12, with the energy-dispersive X-ray (EDX) chemical analysis shown in Table IV. It is possible, therefore, that limited precipitation of carbides may occur on particularly favorable sites during the intermediate cooling stage.

E. *Austenitization Temperature and V_{int}*

Figure 13 shows the effect that the austenitizing temperature has on the sensitivity of the austenite to a low value of V_{int}. Clearly, the differences in critical cooling rate between treatments in which V_{int} = 100 °C s^{-1} and one in which V_{int} = 0.5 °C s^{-1} are most obvious at lower austenitization temperatures (<1100 °C) than at higher temperatures (>1200 °C). However, it is also clear that an increase in the length of the austenitization time to 60 seconds, the sensitivity of the austenite to V_{int} decreases.

The sensitivity of the hardenability to (V_{int} = 0.5 °C s^{-1}) would be expected to increase as the austenitization temperature is reduced, as seen in Figure 13. This is because higher austenitization temperatures will cause more complete homogenization of niobium in the austenite. A more even distribution of niobium throughout the austenite will inhibit the formation of carbides at lower temperatures during cooling by reducing local driving forces for precipitation.

F. *Microstructural Changes Resulting from Varying V_{int}*

Figures 14 and 15 are SEM micrographs of specimens A1 and A2 comparing the microstructures

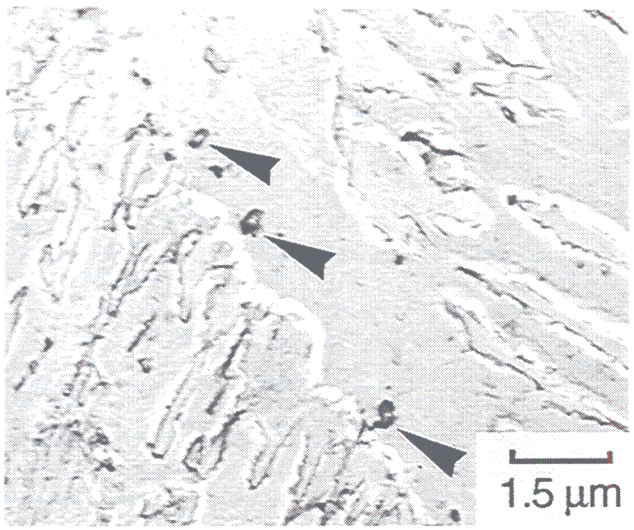

Fig. 12—TEM micrograph from an extraction replica showing the presence of niobium-carbide particles in a specimen cooled at 50 °C s^{-1} following a thermal cycle with T_γ = 1300 °C and V_{int} = 0.5 °C s^{-1}.

Table IV. EDX Chemical Analysis of a Typical Niobium Carbide Particle Present in Steel 1 Following Cooling at 50 °C s^{-1} After a Thermal Cycle with T_γ = 1300 °C and V_{int} = 0.5 °C s^{-1}*

Element	Nb	Fe	Mn	Si	S
Wt pct	94	<1	<1	2	3

*The data do not include carbon or nitrogen; the results are normalized to 100 wt pct.

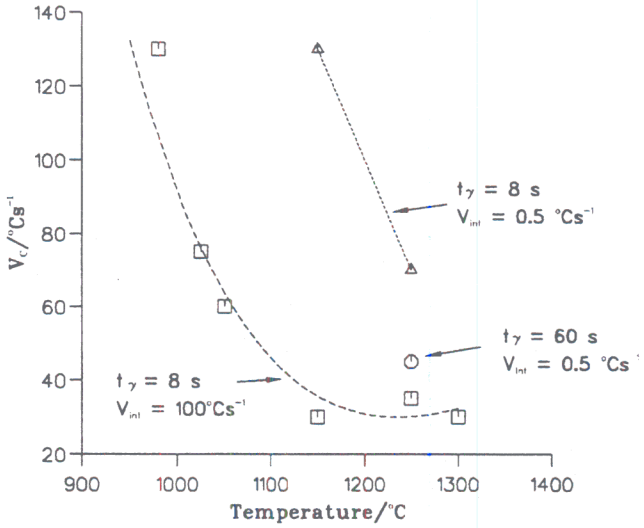

Fig. 13—Comparison of the effect of V_{int} = 100 °C s^{-1} and V_{int} = 0.5 °C s^{-1} on the critical cooling rate as a function of the austenitizing temperature.

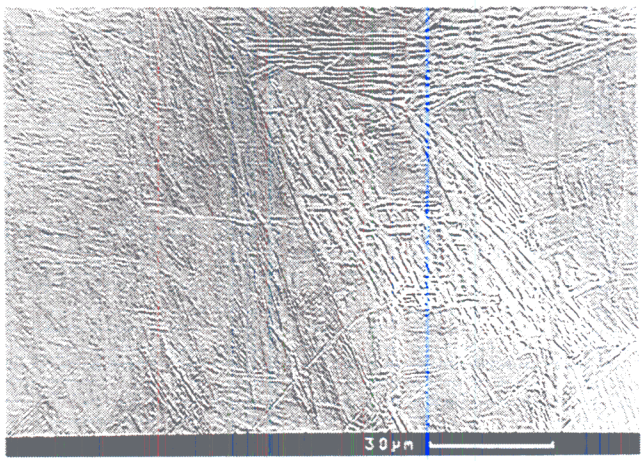

Fig. 14—SEM micrograph of specimen A1 (T_γ = 1250 °C, t_γ = 8 s, and V_{int} = 100 °C s^{-1}).

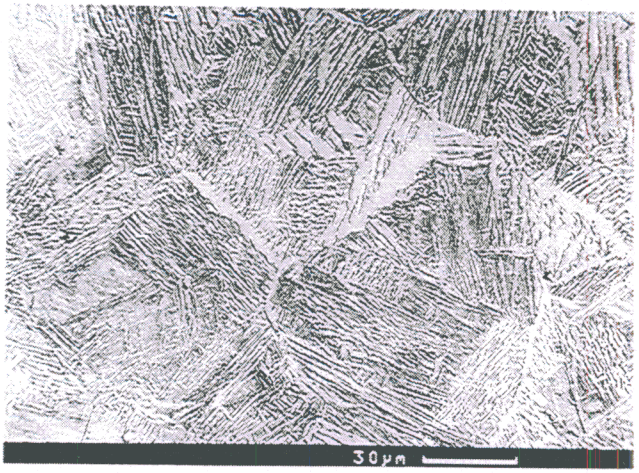

Fig. 15—SEM micrograph of specimen A2 (T_γ = 1250 °C, t_γ = 8 s, and V_{int} = 0.5 °C s^{-1}).

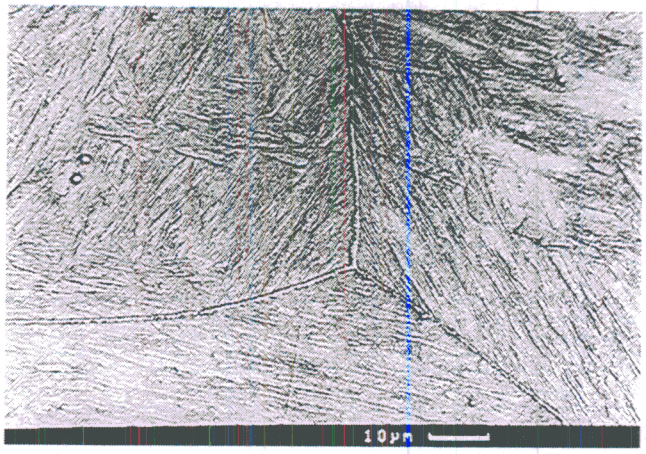

Fig. 16—SEM micrograph of an austenite-grain-boundary triple point decorated with allotriomorphic ferrite after water quenching from 750 °C following heat treatment with V_{int} = 0.5.

produced by cooling at 10 °C s^{-1} following a thermal cycle with T_γ = 1250 °C and t_γ = 8 seconds, but with V_{int} values of 100 °C s^{-1} and 0.5 °C s^{-1}, respectively. The presence of allotriomorphic ferrite in specimen A2 (Figure 15) indicates that transformation initiated at a significantly higher temperature in this specimen than in A1 (Figure 14). Because V_{int} is a measure of the cooling rate between 980 °C and 750 °C, the latter temperature being below Ae_3 for this alloy (Table II), the question arises as to whether or not this ferrite layer formed above 750 °C.

By subjecting a specimen to a heat treatment identical to that experienced by A2 but with the sample water quenched from 750 °C within the simulation chamber of the Thermechmastor, it was observed that some ferrite nucleation does indeed occur above 750 °C, as shown in Figure 16, especially at austenite grain boundary triple points; such regions, however, are extremely rare in the overall microstructure. With V_{int} = 0.5 °C, nucleation therefore occurs above 750 °C, despite the fact that, as shown in Figure 17, there is no detectable volume change above 700 °C when cooling at this rate from 980 °C.

The fact that holding the specimens within the temperature range of niobium-carbide precipitation does have an effect on the transformation of austenite is demonstrated by comparing the micrographs in Figures 18 and 19. These specimens, labeled B1 and B2, were subjected to the heat treatments shown schematically in Figure 20, with the holding times at 950 °C being 0 and 460 seconds, respectively. The temperature 950 °C is well above the Ae_3 temperature of the steel, and therefore there is no possibility of ferrite nucleation before the final cooling stage. Specimen B2 (Figure 19) clearly shows bainite in the microstructure, whereas B1 is fully martensitic.

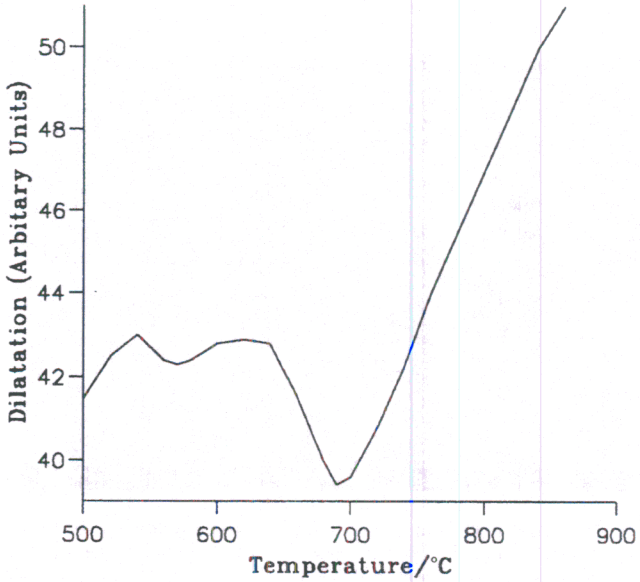

Fig. 17—Dilatometric curve showing that there is no detectable transformation above 700 °C when austenite is cooled at 0.5 °C s^{-1}.

VI. DISCUSSION

A. *Dissolved Niobium and Hardenability*

Many authors have noted the strong retarding effect that niobium has on the transformation of austenite to ferrite, pearlite, and bainite.[6–10] Notably, strong effects are observed when all niobium is in solution. Some authors also report a decrease in hardenability once carbide precipitates can form in the austenite before transformation to ferrite.[10] The origin of this effect must be a retardation of the *kinetics* of austenite decomposition, because the thermodynamic effect of such small quantities of niobium in solution are negligible and, in any case, niobium's effect on the ferrite/austenite equilibrium is to raise the Ae_3 temperature, thereby making it a "ferrite stabilizer."[15]

A comparison of the curves in Figure 9 indicates that the dramatic increase in hardenability observed in steel 1 as the austenitization temperature is increased is the not result of the increase in austenite grain size. The niobium-containing and niobium-free steels show very different relationships between the critical cooling rate and the

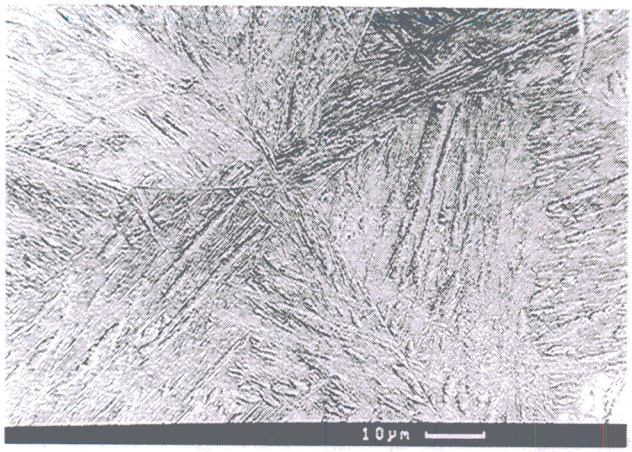

Fig. 18—SEM micrograph of specimen B1 (heat treatment shown in Fig. 20), showing a martensitic structure produced by cooling at 50 °C s^{-1}.

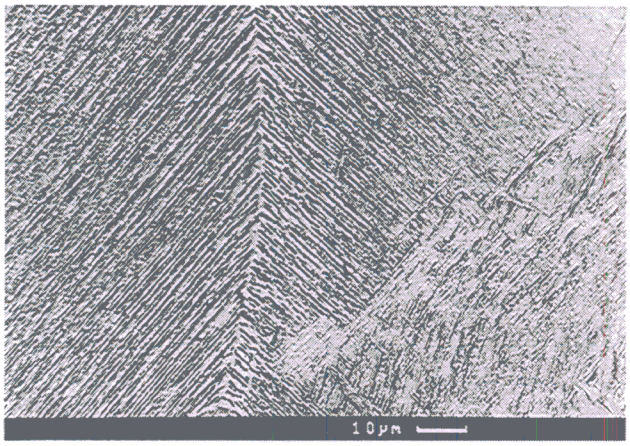

Fig. 19—SEM micrograph of specimen B2 (heat treatment shown in Fig. 20), showing significant quantities of bainite in the microstructure produced by cooling at 50 °C s^{-1}.

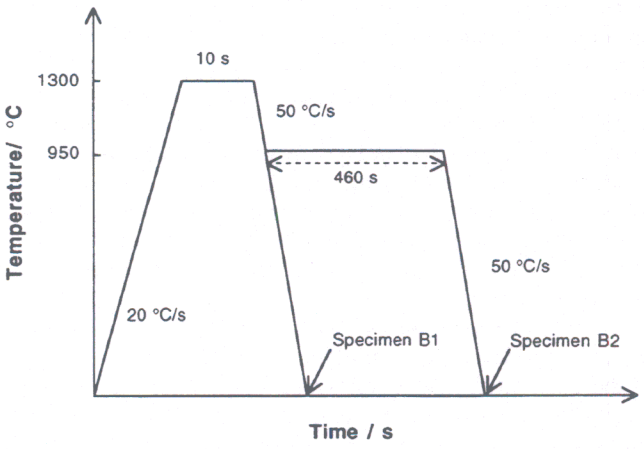

Fig. 20—The heat treatments applied to specimens B1 and B2.

austenite grain size. However, a clear relationship between the calculated dissolved-niobium concentration and the critical cooling rate is observed (Figure 10). We note, however, that for these experiments, as the dissolved-niobium concentration increases, there is a corresponding decrease in the fraction of niobium carbide in the austenite. Significantly, there is close correspondence between the temperature ranges for which the rates of change of both the concentration of niobium in solution and the critical cooling rate are greatest, *i.e.*, just before the particles dissolve completely and rapid grain growth can occur.

These results are consistent with the hypothesis that small amounts of niobium in solid solution strongly retard the decomposition of austenite, but they are also compatible with the observation that the precipitation of niobium carbides can accelerate transformation. A possible effect of niobium in solid solution in steel is that niobium atoms segregate to austenite grain boundaries,[110] where they affect the nucleation of the transformation products of austenite. The mechanism by which the kinetics of transformation are affected is not clear. It has been suggested that because the niobium atoms have a large misfit within the iron lattice,[116,17] austenite grain boundaries are favorable sites for the location of niobium atoms. Interaction of microalloy elements in solid solution with austenite grain boundaries, consistent with segregation resulting from atomic misfit, has been observed,[117,18,19] with significant grain-boundary segregation of titanium measured directly by Miodownick and Martin.[120] Of the common microalloying elements, niobium is reported as interacting most strongly with the boundaries. The reduction in the surface energy of the boundary resulting from such an interaction would decrease its potency as a heterogeneous nucleation site.[121] Using Auger electron techniques, studies of segregation in microalloyed steel by Nachtrab and Chou[122] report no measurements of niobium segregation, although in this case, the analysis was performed on clear areas of boundary, following extensive precipitation of niobium carbonitride. This may have depleted the boundary of any previous enrichment in niobium.

Mechanisms by which the segregation of niobium to austenite grain boundaries where it interacts strongly with carbon have also been proposed.[123] The suggested result of such interaction is that either the local driving force for ferrite formation is decreased or that the diffusion of carbon from ferrite nuclei is hindered. Both effects might lead to a decrease in the nucleation rate of ferrite.

Other explanations for the effect of niobium on the hardenability of steels are less satisfactory, *e.g.*, the suggestion that its presence in solution exerts a "solute drag"[124] on the motion of the ferrite/austenite interface.[110] Such a mechanism would require a concentration spike of niobium to follow the progress of the austenite/ferrite interface in order to retard growth. It has been shown, however, that bainitic ferrite/austenite interfaces show no evidence whatsoever of local solute segregation[125] and that diffusional-solute-drag theory is incompatible with the transformation mechanism of bainite, *i.e.*, formation of plates of ferrite by a displacive transformation.

B. *Slow Cooling between 980 °C and 750 °C*

The observed effect of slow cooling through the temperature range in which niobium carbide precipitates also lends support to the argument that precipitation of niobium carbides at austenite grain boundaries accelerates the transformation of austenite to bainite. Figure 11 indicates that the critical cooling rate is strongly affected by the amount of time that the specimen spends within the temperature range of precipitation. This is entirely expected, because large cooling rates simply do not give sufficient opportunity to precipitate niobium carbides, even at austenite grain boundaries. Limited data also show that austenitizing for longer times decreases the sensitivity of the austenite to this effect (Figure 13).

VII. CONCLUSIONS

A series of heat treatments and corresponding measurements of transformation kinetics indicate that both the allotriomorphic ferrite and bainite transformations in a niobium-microalloyed steel are significantly affected by the distribution of niobium between solid solution and the precipitated state. The observed effect of dissolved niobium on the kinetics of transformation from austenite is consistent with the observation that transformation to bainite is retarded by niobium in solid solution and accelerated by niobium-carbide precipitates.

Our aim in doing this work was to establish the kinetic effect of niobium on low-alloy steel transformations, so that the work can be incorporated into a quantitative model for predicting the heat-affected zone microstructure of welds. In a future attempt, we will incorporate our observations into a TTT curve theory,[26] where the appropriate C curves are displaced according to the niobium concentration, in a manner similar to that already used to model the effect of boron. We also intend to address this problem for other microalloying elements.

APPENDIX

Niobium carbide dissolution kinetics

The equilibrium solubilities (wt pct) of niobium, carbon, and niobium carbide in austenite are described by the familiar solubility product

$$\log [Nb]_{ss}[C]^{n}_{ss} = A - B/T \qquad [A1]$$

where A and B are constants determined experimentally and the integer n represents possible nonstoichiometry in the formula NbC_n.

During rapid continuous heating, only a limited amount of time is available for the diffusion of the carbide-forming elements away from the particles. As the temperature increases such that the solubility of these elements in the matrix exceeds the concentration already in the matrix, the particles begin to dissolve. In these circumstances, complete dissolution is only possible at a temperature where the matrix surrounding the particles can accommodate all of the solute.

Kinetics can be incorporated into this procedure by making the amount of matrix that is available to accommodate the solute time and temperature dependent *via* a diffusion distance calculation. Following,[11] this size r into which niobium atoms can diffuse in time t at temperature T is approximated by

$$r^2 = D\{T\}t \qquad [A2]$$

where $D\{T\} = D_0 \exp\{-Q/RT\}$ is the form of temperature dependence of the diffusion coefficient of the least-mobile species involved in the dissolution process, *i.e.*, niobium in this case. If it is assumed that within the diffusion sphere the niobium achieves the equilibrium concentration given by the solubility product expression, complete dissolution is achieved at a temperature T_s, assuming that the slower diffusing specimens controls the kinetics, where

$$T_s = \frac{B}{A - \log\left(\frac{[Nb]_{ss}[C]}{f}\right)} \qquad [A3]$$

The term f, which defines the effective volume fraction of matrix into which the niobium can dissolve, is given by

$$f = r/l^3 \qquad [A4]$$

where l^3 is the effective total volume of matrix associated with each particle.

For anisothermal conditions, r is estimated using a kinetic strength concept, from

$$r^2 = \int_0^t D_0 \exp\left\{-\frac{Q}{RT\{t\}}\right\} dt \qquad [A5]$$

For linear heating and cooling rates greater than zero, the integral can be expressed as a function of temperature, so that if the initial and final values of r are r_1 and r_2,

$$r_2^2 - r_1^2 = \int_{T_1}^{T_2} \frac{D_0 \exp\left\{-\frac{Q}{RT}\right\}}{V} dT \qquad [A6]$$

where V is the heating or cooling rate for the given linear thermal-cycle section that has start and finish temperatures T_1 and T_2. For isothermal heat treatment, the integration is with respect to time.

The calculated concentration of dissolved niobium, [Nb] is the total concentration that the whole of the matrix can accommodate at equilibrium, whereas $[Nb]_{ss}/f$ represents the local concentration around the dissolving particle. The terms $[C]_p$ and $[Nb]_p$ represent the weight percents of carbon and niobium in precipitate form, and the terms $[C]_t$ and $[Nb]_t$ represent the average niobium and carbon concentrations in the alloy as a whole. It follows that

$$[Nb]_t = [Nb]_{ss} + [Nb]_p \qquad [A7]$$

and

$$[C]_t = [C]_{ss} + [C]_p \qquad [A8]$$

Assuming stoichiometry (NbC, with $n = 1$), we get

$$[Nb]_p = (31/4)[C]_p \qquad [A9]$$

Values of A and B have been given by Reference 13, so that the total amount of niobium in solid solution is given by

$$[Nb]_{ss}^2 + ((31/4)[C]_t - [Nb]_t)[Nb]_{ss} - (31/4) \cdot f \cdot 10^{A-B/T} = 0 \qquad [A10]$$

ACKNOWLEDGMENTS

The authors would like to thank members of the staff at SOLLAC (Dunkerque) who assisted with the experimental work, particularly C. Campione and T. Lemoine. Thanks are also owed to Mr. F. Sauvage and Professor C.J. Humphreys for the provision of laboratory facilities in SOLLAC and Cambridge University, respectively. We would also like to thank Mr. G. Sanz for initiating and sponsoring this collaboration between SOLLAC and the University of Cambridge.

REFERENCES

1. K.E. Easterling: *Mathematical Modelling of Weld Phenomena*, H. Cerjak and K.E. Easterling, eds., Institute of Materials, London, 1993, pp. 183-200.
2. M.F. Ashby and K.E. Easterling: *Acta Metall.*, 1984, vol. 32, pp. 1935-48.
3. W.-B. Li, M.F. Ashby, and K.E. Easterling: *Acta Metall.*, 1986, vol. 34, pp. 1533-43.
4. J. Strid, M.F. Ashby, and K.E. Easterling: *Acta Metall.*, 1985, vol. 33, pp. 2057-74.
5. M.F. Ashby and K.E. Easterling: *Acta Metall.*, 1982, vol. 30, pp. 1969-78.
6. G.T. Eldis and W.C. Hage: *Hardenability Concepts with Application to Steels*, TMS-AIME, Warrendale, PA, 1978, pp. 297-420.
7. D. Webster and J.H. Woodhead: *J. Iron Steel Inst.*, 1964, vol. 202, pp. 987-94.
8. W.B. Morrison: *J. Iron Steel Inst.*, 1963, vol. 201, pp. 317-25.
9. G.L. Fisher and R.H. Geils: *Trans. TMS-AIME*, 1969, vol. 245, pp. 2405-12.
10. M.H. Thomas and G.M. Michal: *Solid-Solid Phase Transformations*, H.I. Aaronson, D.E. Laughlin, R.F. Sekerka, and C.M. Wayman, eds., TMS-AIME, Warrendale, PA, 1981, pp. 469-73.
11. T. Maurickx: Ph.D. Thesis, University of Lille, Lille, France, 1987.
12. B. Sundmann, B. Jansson, and J. Anderson: *CALPHAD*, 1985, vol. 9, p. 153.
13. C. Perdrix, B. Chamont, E. Amoris, and H. Biausser: *IRSID Report*, No. RE 88.322, July 1988.
14. French Standard NF A 04-102, "Produits Sidèrurgiques," Catalogue AFNOR, Paris, 1994.
15. J.S. Kirkaldy, B.A. Thomson, and E.A. Baganis: *Hardenability Concepts with Applications to Steels*, TMS-AIME, Warrendale, PA, 1978, pp. 82-125.
16. F.R. de Boer, R. Boom, W.C.M. Mattens, A.R. Miedema, and A.K. Niessen: *Cohesion in Metals*, Elsevier Science Publishers, New York, NY, 1988, pp. 219 and 385.
17. E.A. Simielli, S. Yue, and J.J. Jonas: *Metall. Trans. A*, 1992, vol. 23A, pp. 597-608.
18. J.J. Jonas and M.G. Akben: *Met. Forum*, 1981, vol. 4, pp. 92-101.
19. S. Yamamoto, C. Ouchi, and T. Osuka: *Thermomechanical Processing of Microalloyed Austenite*, A.J. DeArdo, G.A. Ratz, and P.J. Wray, eds., TMS-AIME, Warrendale, PA 1982, pp. 613-39.
20. M.A. Miodownick and J.W. Martin: *J. Mater. Sci. Lett.*, 1993, vol. 12, pp. 834-35.
21. K.C. Russel: *Acta Metall.*, 1969, vol. 17, pp. 1123-1131.
22. W.T. Nachtrab and Y.T. Chou: *Metall. Trans. A*, 1986, vol. 17A, p. 1995.
23. R.R. de Avillez: Niobium Technical Report, NbTR, 01/82, CBMM, Rio de Janeiro, Brazil, 1982.
24. J.R. Bradley and H.I. Aaronson: *Metall. Trans. A*, 1981, vol. 12A, p. 1729.
25. H.K.D.H. Bhadeshia and A.R. Waugh: *Solid-Solid Phase Transformations*, TMS-AIME, Warrendale, PA 1981, pp. 993-98.
26. H.K.D.H. Bhadeshia: *Met. Sci.*, 1982, vol. 16, pp. 159-65.